Communication

Mesoporous Silica Composites Containing Multiple Regions with Distinct Pore Size and Complex Pore Organization

Anthony Y. Ku, Seth T. Taylor, and Sergio M. Loureiro

J. Am. Chem. Soc., **2005**, 127 (19), 6934-6935• DOI: 10.1021/ja042202r • Publication Date (Web): 23 April 2005

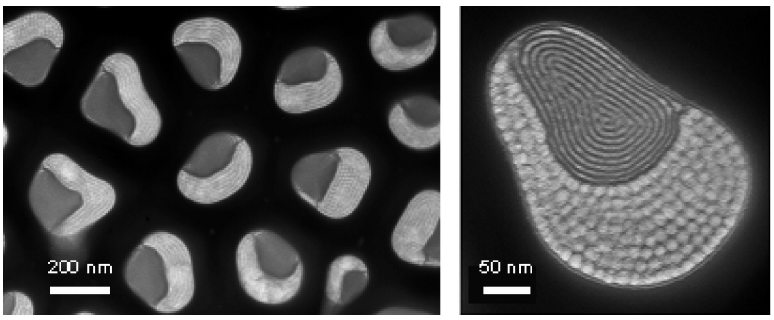

More About This Article

Additional resources and features associated with this article are available within the HTML version:

- Supporting Information
- Links to the 9 articles that cite this article, as of the time of this article download
- Access to high resolution figures
- Links to articles and content related to this article
- Copyright permission to reproduce figures and/or text from this article

View the Full Text HTML

J|A|C|S
COMMUNICATIONS

Published on Web 04/23/2005

Mesoporous Silica Composites Containing Multiple Regions with Distinct Pore Size and Complex Pore Organization

Anthony Y. Ku, Seth T. Taylor, and Sergio M. Loureiro*

General Electric Company, Global Research Center, 1 Research Circle, Niskayuna, New York 12309

Received December 27, 2004; E-mail: loureiro@research.ge.com

Surfactant-templated methods for the synthesis of mesoporous silica have attracted considerable attention since they produce structures with an extraordinary combination of high surface area, narrow pore size distribution, and well-ordered pore organization.[1,2] The pore ordering is especially well-defined in silica where hexagonal close-packed, cubic, lamellar, and bicontinuous disordered pore organizations, such as the L_3 phase, have been reported.[1−3] Most recently, pore size and pore organization have been controlled through a choice of surfactant, introduction of a cosolvent, application of an external field, rigorous control of processing conditions such as temperature and evaporation rate during synthesis, use of a macroporous template, or a combination of the above.[4−12] However, even though surfactant-templated mesoporous ceramic materials can exhibit monodisperse pores ranging from 3 to 50 nm in diameter, the structures produced to date have been limited to a single type of pore size and organization or an uncontrolled mixture of size and organization. It seems clear that further progress in the rational design and synthesis of mesoporous ceramic structures possessing tailored transport properties requires the ability to produce structures with controlled structural heterogeneity at the mesoscopic length scale.

We have overcome this challenge by producing mesoporous silica containing multiple domains with distinct pore size and organization using a multi-stage processing approach schematically depicted in Figure 1. In a typical experiment, a macroporous anodic aluminum oxide membrane (AAO, 200 nm diameter macropores) was immersed in an acidified ethanol-based precursor solution containing a surfactant template and an alkoxide ceramic precursor. Cetyltrimethylammonium chloride (CTAC) and nonionic block copolymers ($EO_{20}PO_{70}EO_{20}$ [Pluronic P123] and $EO_{106}PO_{70}EO_{106}$ [Pluronic F127]) were used as the templates and tetraethoxysilane (TEOS) as the silica precursor. The AAO macropores were filled by evaporation-driven gelation of the precursor solution.[2,9,13] The sample was then heated to 600 °C to remove the surfactant template, shrink the ceramic deposits between growth stages, and allow deposition of additional porous regions. After heating, the membrane was recycled through the process to deposit additional material. Figure 1 also shows a low-magnification plan-view transmission electron microscope (TEM) image of a filled AAO membrane completely filled with the mesoporous silica. Distinct regions corresponding to the different ordering produced by the P123 and F127 templates used in the synthesis are also evident. We observed that the shape of the regions deposited first (darker regions in the image) resembled the shape of the AAO macropore. This suggested complete filling by the gelled material followed by uniform shrinkage during the heat treatment.

Figure 2 shows single-pore plan-view TEM images of samples prepared using different combinations of templates. The images show the different surfactant-templated porosity in each region. In the case of P123- and CTAC-templated regions, the porosity appears as concentric stripes. Detailed analysis of the regions revealed that the pores in these regions were hexagonally-packed channels concentrically wrapped around the axis of the AAO macropore. This is in agreement with the expected ordering of P123-templated regions under confinement.[12] In contrast, the pores in the F127-templated regions appear to be packed in a cubic arrangement. This is consistent with the structure of bulk F127-templated silica.[14]

The pore accessibility of the mesoporous silica composites was examined using nitrogen adsorption measurements, as seen in Figure 2. The adsorption isotherms at 77 K exhibit the characteristic type IV behavior, typical of mesoporous materials. The BET surface areas are listed in Table 1 and ranged from ∼50 to 220 m^2/g

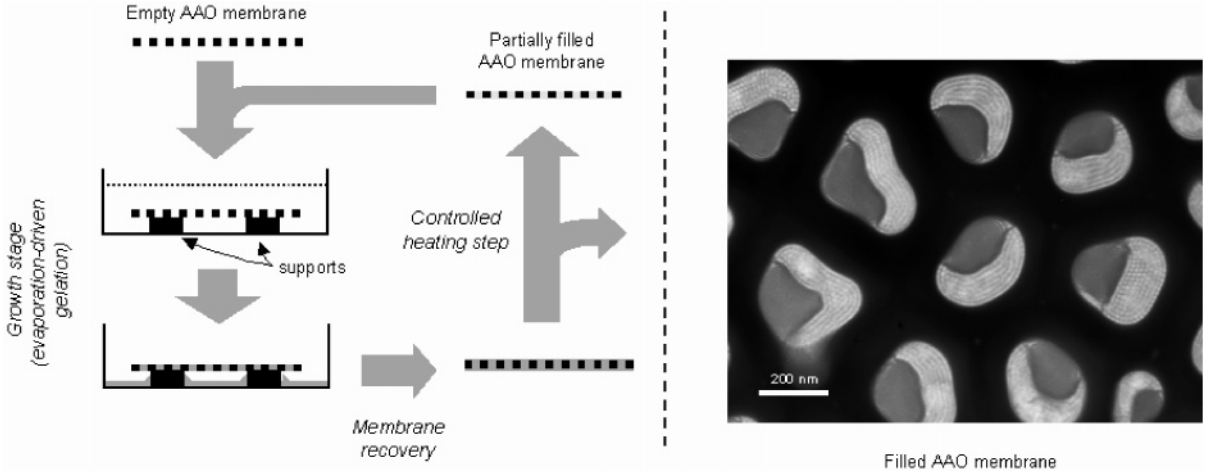

Figure 1. Schematic of the synthesis procedure. Mesoporous silica was grown in the pores of AAO membranes by repeated immersion, gelation, and heating, as shown. Multiple growth steps, using different surfactant templates, were used to sequentially deposit concentric regions with different pore size and organization. A plan view TEM image of an AAO membrane containing mesoporous silica templated using P123 and F127 shows complete filling of the AAO pores.

10.1021/ja042202r CCC: $30.25

Table 1. BET Surface Area and Air Permeability of AAO Membranes Containing Mesoporous Silica. Air Permeability Values Are Reported for Various Membranes at 29 °C and a Pressure Drop of 6.9 kPa

sample	BET surface area (m^2/g)	permeability (10^{-12} mol/m/Pa/s)
control-empty	10	6400
F127−SiO2	220	16
CTAC/F127−SiO2	140	11
P123/F127−SiO2	50	5.6
control-sealed	0	0.1

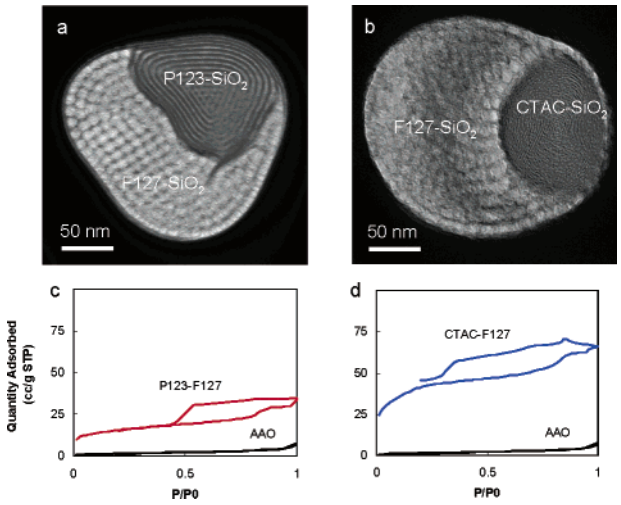

Figure 2. TEM and nitrogen adsorption−desorption isotherms for AAO membranes containing mesoporous silica with complex pore architectures. Different regions with distinct pore organizations can be seen for the (a) P123/F127-templated and (b) CTAC/F127-templated samples. In both cases, the F127-templated region was added during the second growth step. The P123-templated pores are ∼4 nm in diameter, and the CTAC-templated pores are ∼1.5 nm in diameter. The F127-templated regions contain ∼12 nm pores packed in a cubic configuration. Nitrogen adsorption isotherms (c, d) for each sample along with an empty AAO control sample are plotted below the corresponding TEM image.

depending on the relative size and architecture of the mesoporous domains. This overall range agrees with the lower and upper bounds given by empty AAO (∼10 m^2/g) and bulk mesoporous silica powder produced from the gelled material in the bottom of the dish (∼300−600 m^2/g). Although we show detailed results for only two variations, we stress that additional complex architectures were produced using other templates and by varying the order of filling and number of growth steps. These structures will be described elsewhere.

Gas permeability measurements were used to determine if the mesoporous silica completely filled the AAO macropores. Since the permeability scales with nominal pore size,[15] samples with gaps between the AAO wall and the mesoporous silica filler have permeabilities several orders of magnitude higher than those of samples where the AAO pores are completely filled. Table 1 reports air permeability values for AAO containing mesoporous silica as well as control measurements using an empty AAO membrane and an AAO membrane that was completely sealed. The permeability values for the silica-filled AAO membranes were well within the bounds established by the empty and sealed control samples and about an order of magnitude larger than the reported permeability (10^{-12} mol/m/Pa/s) for ∼4 nm mesoporous silica.[16] Our values are larger because the pores in our samples were larger. Furthermore, the permeabilities of samples with gaps (produced using a non-optimized one-step growth process) were on the order of ∼10^{-10} mol/m/Pa/s. The permeability was insensitive to the applied pressure drop over a range of 2000−8000 Pa, suggesting that the mechanism for gas transport was Knudsen diffusion in the completely filled samples.[15]

Mesoporous silica composites with multiple regions of distinct pore size and organization can be systematically synthesized using the approach demonstrated in this paper. Although AAO membranes were used in this work, we expect this approach to be generally applicable to other porous scaffolds. The ability to produce such mesoporous structures is an important step toward the rational design of sensors, filters, and catalysts with integrated functionality and improved performance.

Acknowledgment. This work was supported by the Nanotechnology Advanced Technology program of GE Global Research. We thank M. Blohm and M. Manoharan for technical discussions, J. McKiever for nitrogen adsorption measurements, and S. DeCarr and T. Raber for assistance with the nitrogen permeability measurements. We thank BASF (Mt. Olive, NJ) for providing the block copolymer surfactant templates.

Supporting Information Available: Complete ref 4. This material is available free of charge via the Internet at http://pubs.acs.org.

References

(1) Kresge, C. T.; Leonowicz, M. E.; Roth, W. J.; Vartuli, J. C.; Beck, J. S. *Nature* **1992**, *359*, 710−712.
(2) Yang, P.; Zhao, D.; Margolese, D. I.; Chmelka, B. F.; Stucky, G. D. *Nature* **1998**, *396*, 152−155.
(3) McGrath, K.; Dabbs, D. M.; Yao, N.; Aksay, I. A.; Gruner, S. M. *Science* **1997**, *277*, 552−556; Correction: *Science* **1998**, *279*, 1289.
(4) Vartuli, J. C. et al. *Chem. Mater.* **1994**, *6*, 2317−2326.
(5) Zhao, D.; Feng, J.; Huo, Q.; Melosh, N.; Fredrickson, G. H.; Chmelka, B. F.; Stucky, G. D. *Science* **1998**, *279*, 548−552.
(6) Groenewolt, M.; Antonietti, M. *Langmuir* **2004**, *20*, 7811−7819.
(7) Trau, M.; Yao, N.; Kum, E.; Xia, Y.; Whitesides, G. M.; Aksay, I. A. *Nature* **1997**, *390*, 674−676.
(8) Tolbert, S. H.; Firouzi, A.; Stucky, G. D.; Chmelka, B. F. *Science* **1997**, *278*, 264−268.
(9) Brinker, C. J.; Lu, Y.; Sellinger, A. H.; Fan, A. H. *Adv. Mater.* **1999**, *11*, 579−585.
(10) Yang, P.; Deng, T.; Zhao, D.; Feng, P.; Pine, D.; Chmelka, B. F.; Whitesides, G. M.; Stucky, G. D. *Science* **1998**, *282*, 2244−2246.
(11) Yamaguchi, A.; Uejo, F.; Yoda, T.; Uchida, T.; Tanamura, Y.; Yamashita, T.; Teramae, N. *Nat. Mater.* **2004**, *3*, 337−341.
(12) Wu, Y.; Cheng, G.; Katsov, K.; Sides, S. W.; Wang, J.; Tang, J.; Fredrickson, G. H.; Moskovits, M.; Stucky, G. D. *Nat. Mater.* **2004**, *3*, 816−822.
(13) Melosh, N. A.; Lipic, P.; Bates, F. S.; Wudl, F.; Stucky, G. D.; Fredrickson, G. H.; Chmelka, B. F. *Macromolecules* **1999**, *32*, 4332−4342.
(14) Zhao, D.; Huo, Q.; Feng, J.; Chmelka, B. F.; Stucky, G. D. *J. Am. Chem. Soc.* **1998**, *120*, 6024−6036.
(15) Singh, P. S.; Cussler, E. L. *J. Membrane Sci.* **2001**, *182*, 91−101.
(16) Klotz, M.; Ayral, A.; Guizard, C.; Cot, L. *Sep. Purif. Technol.* **2001**, *25*, 71−78.

JA042202R